Physical Chemistry Chemical Physics

Paper

# Carbon-Contacted Single Molecule Electrical Junctions

Chunhui He,[a,b] Qian Zhang,[a,b] Shuhui Tao,[a,b] Cezhou Zhao,[c] Chun Zhao,[c] Weitao Su,[d] Yannick J. Dappe,[e] Richard J. Nichols,[b] Li Yang*[a,b]

Received 00th January 20xx,
Accepted 00th January 20xx

DOI: 10.1039/x0xx00000x

**www.rsc.org/**

A fully metal-free molecular junction (MJ) has been built by using electrochemically etched carbon fibre STM tip as top electrode and graphene as bottom electrode. The corresponding conductance values for 1,n-alkanediamine and 1,n-alkanedithiol (n=2, 4, 6, 8, 10) have been measured using the STM-*I*(*s*) technique. The tunneling decay constant of the alkanediamine and alkanedithiol junctions with these carbon contacts is much lower than the corresponding metal contacted junctions at 0.24 and 0.38 per (-$CH_2$) unit, but the junction conductance with carbon contacts is also lower. The carbon fibre tip can be considered to a good candidate as an electrode. Compared with the gold tip, the carbon fibre tip leads to correspondingly lower molecular junction conductance.

## Introduction

Single-molecule junctions (MJs) have provided new opportunities for studying in a highly defined manner charge transfer across molecular bridges.[1] Several techniques have been developed for making electrical measurements on MJs, such as mechanically controlled break junctions (MCBJ) [2], conductive probe atomic force microscopy (CP-AFM) [3], scanning tunnelling microscopy break junctions (STM-BJ)[4] and the *I*(*s*) technique[5] based on STM. To date, gold has been the main material of choice for single-molecule electronic measurements, since gold offers good chemical stability, high conductivity and ease of fabrication of MJs.[6] Using gold electrodes, many types of MJs have been studied, which has included the deployment of different anchoring groups, for example, thiol (-SH)[7], amine (-$NH_2$)[7, 8], carboxylic acid (-COOH)[7] or isocyanide (-NC)[9] groups. However, gold electrodes also have several disadvantages, such as mobility of surface atoms at room temperature and in this case of integration with conventional semiconductor devices a poor compatibility with complementary metal oxide semiconductors. Furthermore, MJs with metal electrodes such as Au, Ag, and Pt can also exhibit thermal fluctuations arising from metal atom mobility and instabilities.[10] In this respect it is important that research in single molecule electronics also addresses the challenges of other contact materials, which will ultimately affect the implementation in molecular electronics devices. Recently, it has become possible to make reliable single molecule electrical measurements with other non-metallic contacts such as carbon-based materials, with carbon-based electrodes representing a first step towards all-carbon single molecule electronics.[11] A technical challenge here is to produce MJs using carbon-based electrodes with high yield, good reproducibility, and excellent stability and to exploit their lower tendency for atom migration than the more "fluid" metallic contacts.[12] Guo *et al*.[13] have described a method to wire molecules into gaps with single walled carbon nanotubes. They then demonstrated that the single-molecule conductance of these carbon-contacted junctions exhibited different behaviour to junctions contacted to metal electrodes, with molecule bridges connecting or breaking depending on the solution pH. Li *et al*.[14] have shown that chemically derived graphene films can be applied directly as a top contact electrode and that graphene can be also used as the conductive interlayer to protect self-assembled monolayers. Jia *et al*.[15] used double graphene electrodes and diarylethene to form a stable MJ with conductivity which could be reversibly photoswitched between high and low states. Supur et al.[16] fabricated the large-area molecular electronic junctions consisting of 5-carbon wide graphene ribbons between two carbon electrodes.

[a] *Department of Chemistry, Xi'an-Jiaotong Liverpool University, 215123, Suzhou, China. E-mail: li.yang@xjtlu.edu.cn*
[b] *Department of Chemistry, University of Liverpool, Liverpool, L69 7ZD, UK.*
[c] *Department of Electrical and Electronic Engineering, Xi'an-Jiaotong Liverpool University, 215123, Suzhou, China*
[d] *College of Materials and Environmental Engineering, Hangzhou Dianzi University, 310018, Hangzhou, China*
[e] *SPEC, CEA, CNRS, Université Paris-Saclay, CEA Saclay 91191 Gif-sur-Yvette Cedex, France*

In our previous works[17-19], we reported that the use of graphene to replace top electrodes reduces drastically the current attenuation factor in the MJs. Here, we extend this to build a fully metal-free MJ by using carbon fibre as the top electrode, and graphene as the bottom electrode. Carbon fibre possesses positive attributes such as good hardness, high breaking strength, good chemical stability and high temperature stability. These outstanding properties have made carbon fibre extremely popular in aerospace, civil engineering, military, and motorsports.[20] Rubio-Bollinger et al.[21] have demonstrated that carbon fibre tips can be used to form single molecule junctions by using STM-BJ technique. They used a mono-functionalised octanethiol with the thiol forming a thiolate contact to a gold substrate and made contact through the terminal methyl group to the carbon tip.[12,21]

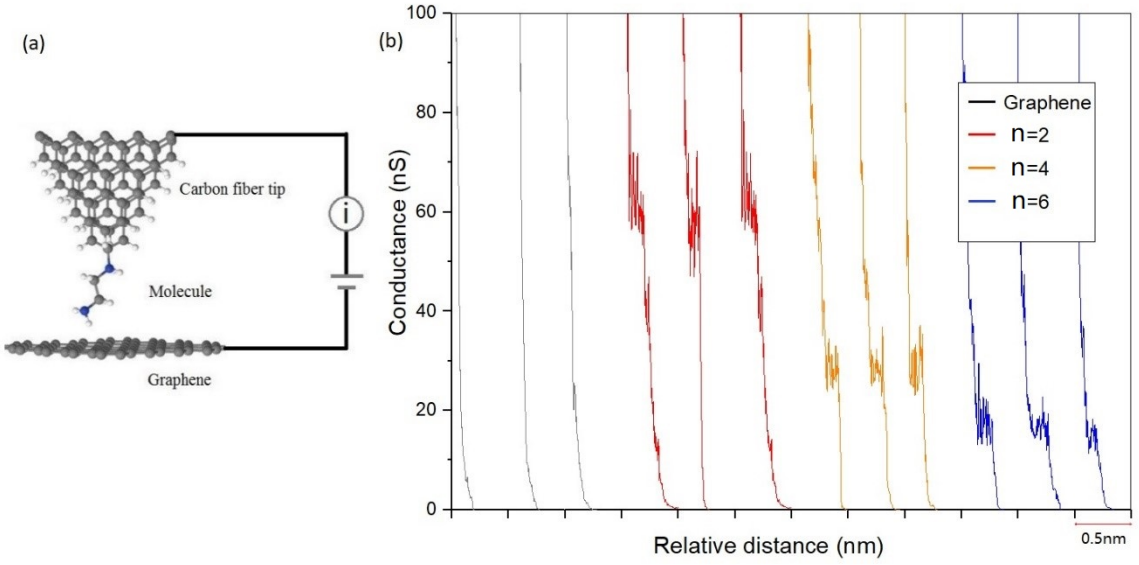


**Figure 1**. (a) Schematic diagram of the molecular junction formed in this study. (b) Typical *I*(*s*) curves of 1,n-alkanedithiols, with n=2 (red), 4 (orange) and 6 (blue). The black curves are recorded in the absence of molecules of on graphene.

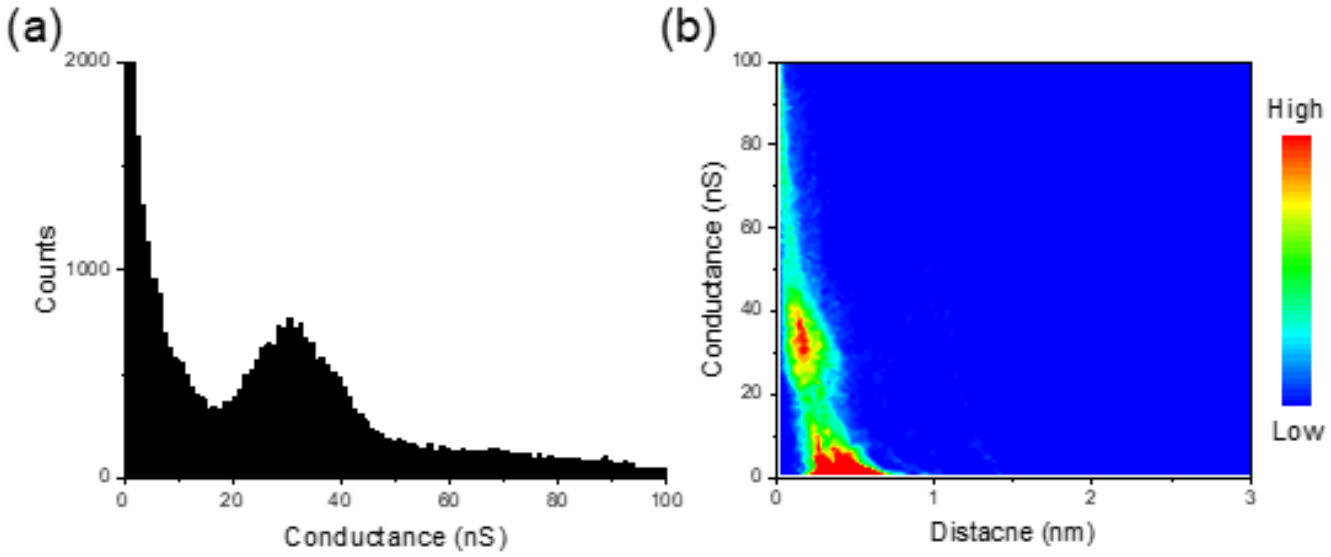


 

**Figure 2**. (a) A 1D histogram of single-molecule conductance of carbon fibre−1,4-butanedithiol (n=4)−graphene hybrid junctions (b) The corresponding 2D histogram where red represents high point count.

In the present work, we demonstrate that MJs can be formed by using graphene and a carbon fibre electrode as the respective contacts. The conductance values of 1,n-alkanediamine and 1,n-alkanedithiol (n=2, 4, 6, 8, 10) have been measured by using the STM-*I*(*s*) technique. In addition, we have investigated the length dependence of conductance of these molecules with the decay constant (βn) being experimentally determined across the n = 2 to 10 series, which we have compared with literature values for Au-molecule-graphene junctions and Au−molecule−Au junctions. The carbon tip is found to behave very similarly to the gold tip, with however a lower conductance, but also a slightly smaller attenuation factor, in particular for the diamine case.

## Methodology

A few layer thick graphene on nickel substrates (10 mm×10 mm) were purchased from The Graphene Supermarket (USA) and used as the bottom electrode. Top electrodes were fabricated from carbon fibre tips by electrochemical etching of 0.3 mm diameter carbon fibre rod (Toray Industries).[22] Molecular adsorption to graphene substrate was generally achieved by immersing the graphene substrate into molecular solutions (molecule −methanol, 1:20, v/v) for 90 s. The conductances of 1,n-alkanediamine and 1,n-alkanedithiol (n=2, 4, 6, 8, 10) in the junctions were measured by using STM-based *I*(*s*) technique[5] (Bruker EC-STM). The STM-*I*(*s*) measurements were made by performing distance retraction scans from 0 to 3 nm relative to the current setpoint, with a bias voltage of 0.3 V and the ramp rate was 1.03 Hz.

Over 500 current-distance curves exhibiting characteristically stepped plateaus were selected for further data analysis. The one dimensional (1D) and two dimensional (2D) histograms were then plotted for determination of the molecular conductance.

## Results

The *I*(*s*) technique (*I* = current and *s* = distance during the STM tip retraction) was used to characterize carbon fibre−molecule−graphene junctions by measuring the single-molecule conductance. The typical setup is illustrated in Figure 1a with the corresponding unit cell used in the calculations. Experimentally in the single molecule junction, we are unable to determine the precise bonding at each contact so we have to assume the bonding configurations at the contacts and then compare our computational results with the experimental observations, as is often the case in single molecule electronics studies. In both the thiol and amine terminated junctions, the carbon fibre tip (modelled as a stack of three graphene nanoribbons of triangular shape, see Ref[11] for more details) contacts covalently the molecule. In particular, the sulfur is contacted by removing the hydrogen of the thiol group, as commonly occurs in the case of a gold-thiol interaction, whereas the nitrogen keeps its two hydrogen atoms and becomes then slightly positively charged, as it is well known for tetravalent nitrogen. On the other side, the graphene electrode contacts the molecule through weak van der Waals interactions. As we have proven previously[18,19] and we will see here also, the asymmetry of interactions at the contacts is responsible for the peculiar electronic behaviour of the junction. **Figure 1b** shows two different types of typical conductance−distance curves for 1,n-alkanedithiol junctions: one type is a pure exponential decay if the tip retracts from the substrate without a molecule bridging between tip and substrate (black curves), while the another type features plateaus due to the formation of molecular junctions (red, yellow, blue, orange and purple curves). At larger distances (s) in the retraction there is a sudden drop (step) in the decay curves which corresponds to the breaking of the molecular junctions. As expected, the corresponding junction conductance values decrease with the molecular length for each series of molecules. For example, the conductance of carbon fibre−1,2-ethanedithiol−graphene junctions is located at around 50-75 nS. By contrast, the plateaus of carbon fibre−1,4-butanedithiol−graphene junctions and carbon fibre−1,6-hexanedithiol−graphene junctions decrease in a stepwise fashion, located between 25 nS to 40 nS and 10 nS to 20 nS, respectively.

In order to obtain a reliable determination of junction conductance, for each system a large number of current-distance traces must be repetitively collected and then these must be statistically analysed. Over 500 *I*(*s*) scans containing a clear plateau were used in the

histogram analysis to find the most dominant location of the conductance. In Figure 2(a) a significant peak was observed in the histogram for carbon fibre-1,4-ethanedithiol-graphene junctions, which indicates the most probable molecular value. Using a Gaussian fit of this peak, the obtained conductance value is 32 nS. The corresponding 2D histogram shown in Figure 2(b) display simultaneously the distribution of conductance values and the length of the molecular junction. A red region (high point count) located around 25 nS to 40 nS is clearly observed in the 2D histogram which is consistent with the peak in Figure 2(a) and the plateaus shown in Figure 1(b). Figure 3a presents conductance histograms of carbon fibre-1,n-alkanedithiol-graphene junctions (n = 2, 4, 6, 8, 10) with the same counts scale and conductance. Only a single main peak can be found in each histogram, and the conductance values of 1,2-ethanedithiol (n=2) (black),1,4-butanedithiol (n=4) (blue), 1,6-hexanedithiol (n=6) (red), 1,8-octanedithiol (n=8) (green) and 1,10-decanedithiol (n=10) (purple) are measured as 64, 32, 17, 6, and 3 nS, respectively. **Figure 3b** shows the conductance values of 1,2-ethanediamine (n=2) (black),1,4-butanediamine (n=4) (blue), 1,6-hexanediamine (n=6) (red), 1,8-octanediamine (n=8) (green) and 1,10-decanediamine (n=10) (purple) are 66, 30, 23, 15 and 6.3 nS. As expected, the conductance of 1,n-alkanediamine/1,n-alkanedithiol decreases as the length of the molecule increases.

Typically, molecules shorter than 3-5 nm with wide HOMO-LUMO gaps are considered to conduct through non-resonant tunnelling mechanisms, with in the most straightforward cases the conductance decreasing exponentially with the molecular length.[23] On another hand, a weaker dependence of conductance on molecular length is typically predicted if hopping mechanisms prevail which is more likely to be the case for longer molecular lengths and molecular bridges with defined hopping sites.[24] In either case, investigating the length dependence of the molecular conductance can give insight into the transport mechanism. In the present case, the conductance in this regime can be described by $G = A \exp(-\beta_n n)$, where $G$ is the conductance; A is typically related to the nature of the molecule−electrode interaction, which reflects the contact resistance; $\beta_n$ is the decay constant per number of ($-CH_2$) units, which describes the efficiency of electron transport through the molecules; and $n$ is the number of methylene groups. From the natural logarithmic plot of the conductance versus the number of ($-CH_2$) units in Figure 4, the tunnelling decay constant of the carbon fibre-1,n- alkanedithiol(amine) -graphene structure is 0.38 (0.24), which is a surprisingly low value compared to the case of the gold- 1,n-alkanedithiol (amine)-gold configuration.

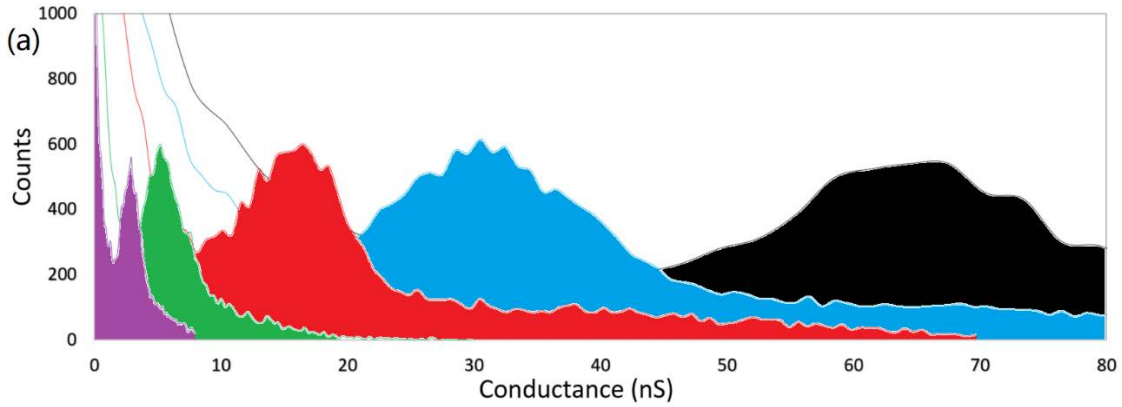

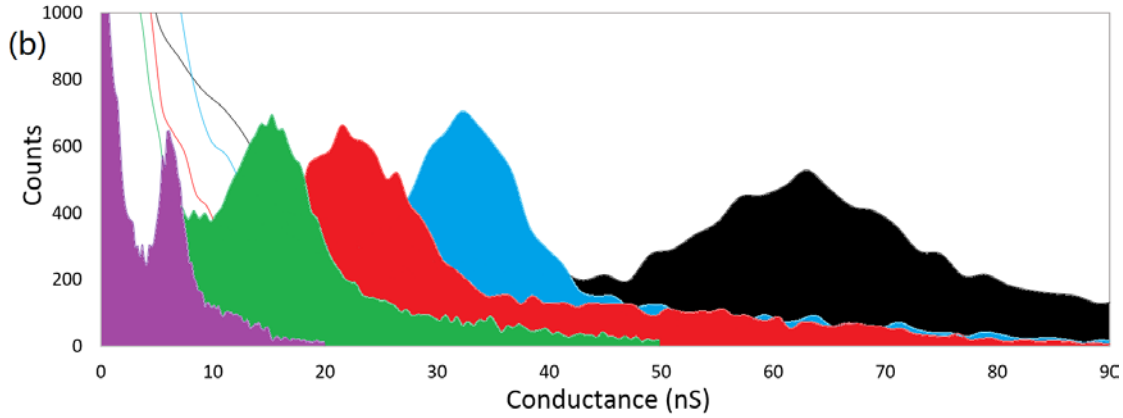


**Figure 3**. Conductance histograms for (a) carbon fibre-1,n-alkanedithiol –graphene junctions in which n = 2 (black), 4 (blue), 6 (red), 8 (green), and 10 (purple). (b) carbon fibre-1,n-alkanediamine–graphene junctions in which n = 2 (black), 4 (blue), 6 (red), 8 (green), and 10 (purple).

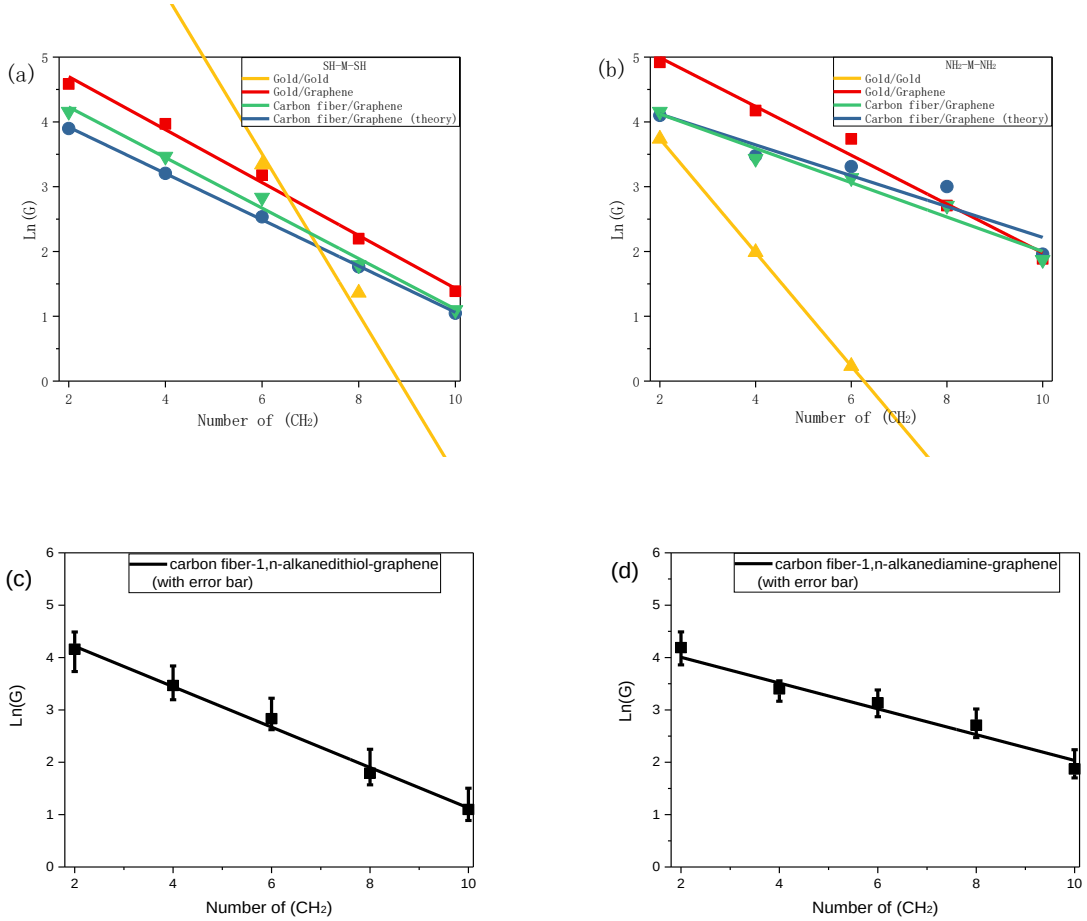


**Figure 4**. Natural logarithmic plot of the conductance as a function of the number of $CH_2$ groups for (a) the 1,n-alkanedithiol homologous series, (b) for the 1,n-alkanediamine series, (c) for carbon fibre-1,n-alkanedithiol-graphene junctions with error bars and (d) for carbon fibre-1,n-alkanediamine-graphene junctions with error bars.

**Table 1:** Conductance values and tunnelling decay constant for SH-$(CH_2)_n$-SH and $NH_2$-$(CH_2)_n$-$NH_2$ with different electrodes.

| Molecular junctions | Conductance(nS) | | | | | Tunnelling decay constant ($\beta_n$) | Contact resistance (MΩ) |
|---|---|---|---|---|---|---|---|
| | n=2 | n=4 | n=6 | n=8 | n=10 | | |
| Carbon fibre-S-$(CH_2)_n$-SH-Graphene | 64 | 32 | 17 | 6 | 3 | 0.38±0.02 | 6.8±0.7 |
| Carbon fibre-S-$(CH_2)_n$-SH-Graphene (theory) | 49.28 | 24.46 | 12.61 | 5.84 | 2.85 | 0.39 | |
| Au-S-$(CH_2)_n$-SH-Graphene | 98 | 53 | 24 | 9 | 4 | 0.40[18] | 3.9 |
| Au-S-$(CH_2)_n$-SH-Au | - | - | 28.2 | 3.9 | 0.2 | 1.08(LC)[7, 25] | |
| Carbon fibre-$NH_2$-$(CH_2)_n$-$NH_2$-Graphene | 64 | 31 | 23 | 15 | 6.5 | 0.24±0.03 | 11.1±2.2 |
| Carbon fibre-$NH_2$-$(CH_2)_n$-NH2-Graphene (theory) | 60.3 | 32.37 | 27.40 | 20.12 | 7.09 | 0.23 | |
| Au-$NH_2$-$(CH_2)_n$-$NH_2$-Graphene | 137 | 65 | 42 | 15 | 6.6 | 0.37[19] | 3.7 |
| Au-$NH_2$-$(CH_2)_n$-$NH_2$-Au | 42 | 7.3 | 1.26 | - | - | 0.81(LC)[7] | |

**Table 1** summarizes conductance values and tunnelling decay constants of 1,n-alkanedithiol/1,n-alkanediamine obtained experimentally and theoretically with different electrodes. Interestingly, the conductance values for non-metallic contacts in 1,n-alkanedithiol junctions are smaller compared to the ones obtained in the case of a gold-gold molecular junction. For example, it was found *G* = 23 nS and 17 nS for gold−1,6-hexanedithiol (n=6)−graphene junctions and carbon fibre−1,6-hexanedithiol (n=6)−graphene junctions, respectively. For the carbon fibre-1,n-alkanedithiol(amine)-graphene series we observe that contact resistance is 6.8/11.1 MΩ, which is much higher than that obtained for gold-1,n-alkanedithiol (amine)-graphene (3.9/3.7MΩ). The present beta values, where both the contacts are carbon, are similar to the one obtained in our previous work[18] on 1,n-alkanedithiol molecular bridges with one graphene and one gold contact. For example, our measurements on fully non-metallic MJs yield $\beta_n$ = 0.38 per (-$CH_2$) unit, which as shown in **Table 1**, is much smaller than that obtained using a pair of gold electrodes ($\beta_n$=1.08). However, this value is only slightly smaller than the $\beta_n$ value obtained for gold-1,n-alkanedithiol-graphene junction ($\beta_n$=0.40). In the latter case, the attenuation factor was mainly driven by the symmetry breaking induced by the graphene electrode (namely the difference of coupling at each interface, covalent bonding with the gold electrode and vdW bonding with the graphene electrode). This arises since the electrostatic dipole at the graphene-molecule interface is much weaker than the dipole at the gold-molecule interface. This results in a significant charge transfer at the gold-molecule interface, with the important consequence of this being a reduction in the electronic barrier at the interface responsible for the attenuation factor.[26] Regarding 1,n-alkanediamine bridges, the present $\beta_n$ values are somewhat smaller than those obtained in our previous work for graphene-molecule-gold junctions,[19] but much larger than values obtained for gold-gold molecular junction. Overall, the attenuation factor is even smaller, with $\beta_n$ = 0.24 per (-$CH_2$) unit. In the case of

 

the gold-1,n-alkanediamine-graphene configuration, graphene also induces a symmetry breaking

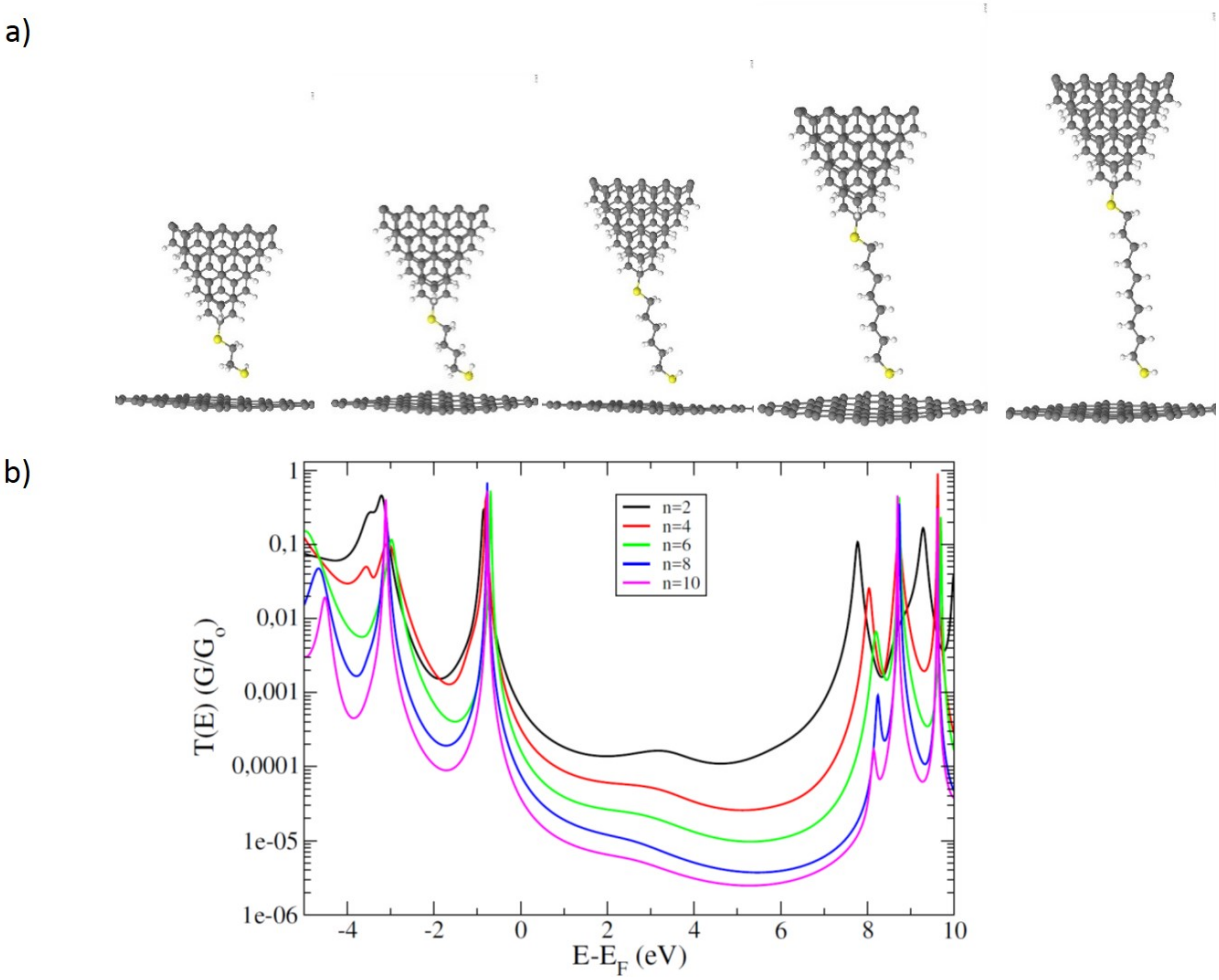


**Figure 5.** (a) Optimized atomic configurations of our model carbon fibre tip-1,n-alkanedithiol-graphene molecular junctions and (b) corresponding electronic transmissions.

by splitting the HOMO level. Hence, the new HOMO level location results in an equal reduction of the electronic barrier compared to the reduction of the electronic barrier between the gold-gold and gold-graphene alkanedithiol junctions. The main difference between alkanedithiol and alkanediamine junctions lies in the coupling of the anchoring groups: the sulfur atom couples well with the electrodes (which justifies the small electronic barrier) but poorly to the molecular backbone. Oppositely, the amine group couples poorly to the electrode (which explains the higher electronic barrier, around 3.5 eV), but couples very well to the molecular backbone, ensuring a good conductance in the junction. Consequently, the electronic transport in both junctions results from an interplay between coupling to the electrode (electronic barrier) and coupling to the molecular backbone. This interplay yields the same attenuation factor for both junctions.[25]

In order to understand these similar trends obtained using the carbon tip, we have performed Density Functional Theory (DFT) calculations to determine the equilibrium geometry of the different junctions, as well as their electronic structure, and subsequently determined the junction electrical current by using a Keldysh-Green formalism following a well-established procedure.[18,19] As a model for the carbon fibre tip, we have used a previously deployed three-layer graphene tip, whose potential for all-carbon molecular junctions[11] or STM tips[27] has been theoretically demonstrated. It has to be noted that while the carbon tip is hydrogenated for stability reason, the

apex hydrogen is removed when contacting the molecular chain, leading to a covalent bond with the molecule. In **Figure 5**, we present the optimized atomic configuration for the different 1,n-alkanedithiol chains, as well as the corresponding calculated electronic transmissions.

From these transmissions, we can deduce that the electronic transport in the 1,n-alkanedithiol molecular junctions is driven by the HOMO level of the molecules, since we can observe a strong transmission peak located at around 0.7 eV below the Fermi level. To determine the attenuation factor, we consider a previously used simple tunnelling model, namely $\beta_n = 2d_0\sqrt{(2m\varphi)}/\hbar$ [28], where $d_0$ is the unit length between the monomers in the molecule, $m$ is the mass of the electron, and $\varphi$ is the barrier height, *i.e.* $E_F$-$E_{HOMO}$. In this case, the attenuation factor is found to be $\beta_n \sim 0.5$ per (-$CH_2$) unit, which is larger than the experimentally obtained value. This can be compared with the Au-1,n-alkanedithiol-graphene molecular junctions, where $\beta_n$ was found to be 0.4 per (-$CH_2$) unit ($E_F$-$E_{HOMO}$ being 0.4 eV). It is well known that the Au-S interaction and therefore the charge transfer at that interface is slightly overestimated in the DFT

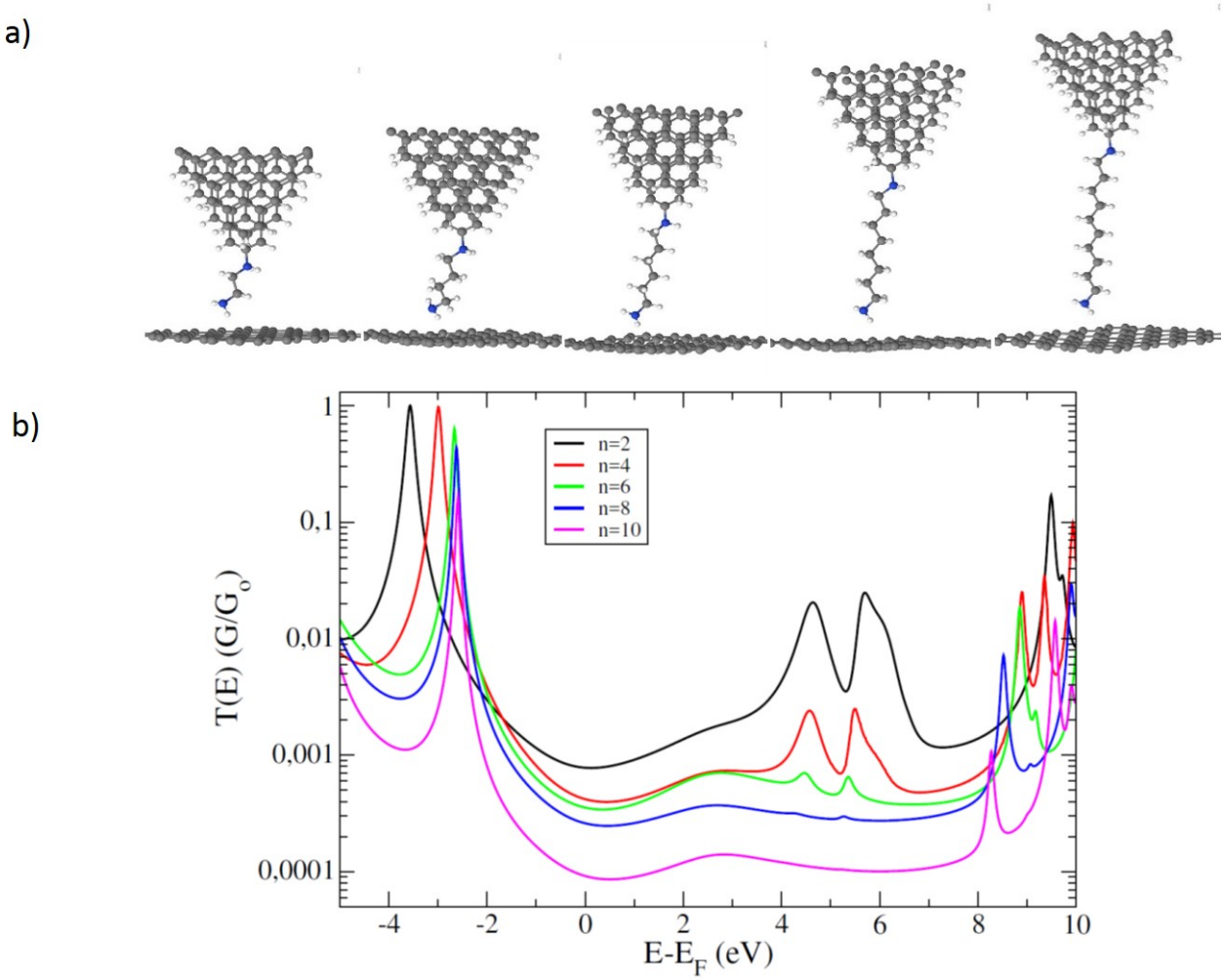


**Figure 6.** (a) Optimized atomic configurations of our model carbon fibre tip-1,n-alkanediamine-graphene molecular junctions and (b) corresponding electronic transmissions.

calculations. Consequently, if the HOMO level positions in the Au-1,n-alkanedithiol-graphene and carbon fibre tip-1,n-alkanedithiol-graphene molecular junctions are located approximately at the same position (between 0.4 and 0.7 eV below the Fermi level), the

resulting attenuation factor will be the same, around 0.4 per (-$CH_2$) unit, which is in reasonably good agreement with $\beta_n$ values observed experimentally. Hence, in the case of 1,n-alkanedithiol chains, we can conclude that the carbon tip "behaves like a gold tip", leading to the same attenuation factor, but with however a slightly reduced junction conductance.[11]

We now consider the case of the 1,n-alkanediamine based molecular junctions. As explained by Zhang *et al* [19], the simple barrier tunnelling model where $\beta_n = 2d_0\sqrt{(2m\varphi)}/\hbar$ [28], is not sufficient to explain the low attenuation for 1,n-alkanediamine molecular junctions. In this case, the attenuation factor is determined by an interplay between the electronic properties of the isolated molecule and the interface properties, due to a better coupling of the amine group with the molecular backbone, which is opposite to the thiol group, which couples better to the electrode. For the dithiol case, the HOMO orbital is strongly localized on sulfur atoms, while it spreads significantly into the backbone chain for the diamine case.[19]. In **Figure 6**, we represent the optimized atomic configuration for the different 1,n-alkanediamine chains, as well as the corresponding calculated electronic transmissions. In this case, we obtain a situation very similar to the case of the gold-1,n-alkanediamine-graphene junctions, with a HOMO level located at around 3.5 eV below the Fermi level[19]. In that junction, the attenuation factor was estimated to be around 0.3-0.4 per (-$CH_2$) unit. In the present case, using the carbon tip which yields a similar electronic barrier, the attenuation factor observed experimentally is estimated at around 0.24 per (-$CH_2$) unit, a bit lower due to a slightly closer HOMO level, but which is consistent with our previous findings on gold-1,n-alkanediamine-graphene junctions.

Finally, the electronic gap in these carbon tip-1,n-alkanediamine-graphene molecular junctions is now found to be around 7 eV, which is much smaller than in the gold-1,n-alkanediamine-gold case (~ 11 eV) and even in the gold-1,n-alkanediamine-graphene (~ 9.5 eV) case. Therefore, since the coupling to the electrodes varies as the inverse of the gap through self-energy calculations, the conductance in the carbon tip-1,n-alkanediamine-graphene junction should be higher than in the two latter cases. However, since the carbon tip-molecule interface is less conductive than the gold tip-molecule interface, the transmission is reduced through the electrode. As a consequence, the conductance of the carbon tip-1,n-alkanediamine-graphene junction is found to be higher than in the gold-1,n-alkanediamine-gold, as previously observed for the gold-1,n-alkanediamine-graphene junction.[19] However, the conductance of carbon tip-1,n-alkanediamine-graphene junction is still smaller than the gold-1,n-alkanediamine-graphene junction due to the reduced conductance of the carbon tip-molecule interface.

## Conclusions

We present here a combined experimental and theoretical study of the use of all-carbon molecular junctions. We have studied 1,n-alkanedithiol and 1,n-alkanediamine chains trapped between a graphene electrode and a carbon fibre tip. In both cases, we find similar behaviours as when using a standard gold electrode instead of the carbon tip, due to the symmetry breaking induced by graphene in those systems, namely with a covalent contact to the tip and a van der Waals contact to graphene. Indeed, for the 1,n-alkanedithiol chain, the attenuation factor is found to be the same, around 0.4 per (-$CH_2$) unit, with smaller conductance values due to the lower electronic transmission of the carbon tip-molecule interface. For the 1,n-alkanediamine molecular bridge with carbon fibre tips and graphene bottom electrodes, we also obtain a similar behaviour to that obtained using a gold tip with graphene. However, a higher conductance is obtained with respect to the 1,n-alkanedithiol junction. The 1,n-alkanediamine junction gives the lowest length decay of the conductance but the gain here is offset by the lower transmission of carbon tip-molecule interface. However, the low decay could be promising for junctions of alkane chain backbone longer than ten methylene units. To conclude, the carbon tip-1,n-alkanediamine-graphene molecular junction generally behaves like the previously studied gold-1,n-alkanediamine-graphene molecular junction, with slightly smaller conductances, but also a smaller attenuation factor.

## Conflicts of interest

There are no conflicts to declare.

## Acknowledgements

This work was supported by the National Natural Science Foundation of China (NSFC Grants 21503169, 2175011441), Jiangsu Human Resource and Social Security Grant (2014-XCL-038), Suzhou Science and Technology programme (SYG 201623), Suzhou Industrial Park Initiative Platform Development for Suzhou Municipal Key Lab for New Energy Technology (RR0140), Key Program Special Fund in XJTLU (KSF-A-04 and KSF-A-07) and the XJTLU Research Development Fund (RDF-14-02-42).

## Notes and references

1. Y. Cao, S. Dong, S. Liu, L. He, L. Gan, X. Yu, M. L. Steigerwald, X. Wu, Z. Liu and X. Guo, *Angewandte Chemie*, 2012, **51**, 12228-12232.
2. M. A. Reed, C. Zhou, C. J. Muller, T. P. Burgin and J. M. Tour, *Science*, 1997, **278**, 252-254.
3. X. D. Cui, A. Primak, X. Zarate, J. Tomfohr, O. F. Sankey, A. L. Moore, T. A. Moore, D. Gust, G. Harris and S. M. Lindsay, *Science*, 2001, **294**, 571-574.
4. B. Xu and N. J. Tao, *Science*, 2003, **301**, 1221-1223.
5. W. Haiss, H. V. Zalinge, S. J. Higgins, D. Bethell, H. Höbenreich, D. J. S. And and R. J. Nichols, *Journal of the American Chemical Society*, 2003, **125**, 15294-15295.
6. L. Liu, Q. Zhang, S. Tao, C. Zhao, E. Almutib, Q. Al-Galiby, S. W. Bailey, I. Grace, C. J. Lambert, J. Du and L. Yang, *Nanoscale*, 2016, **8**, 14507-14513.
7. F. Chen, X. Li, J. Hihath, Z. Huang and N. Tao, *Journal of the American Chemical Society*, 2006, **128**, 15874-15881.
8. S. Y. Quek, H. J. Choi, S. G. Louie and J. B. Neaton, *Nano Letters*, 2009, **9**, 3949-3953.
9. B. Kim, J. Beebe, Y. Jun, X. Y. Zhu and C. D. Frisbie, *Journal of the American Chemical Society*, 2006, **128**, 4970-4971.
10. H. Yan, A. J. Bergren and R. L. Mccreery, *Journal of the American Chemical Society*, 2011, **133**, 19168-19177.
11. Y. J. Dappe, C. Gonzalez and J. C. Cuevas, *Nanoscale*, 2014, **6**, 6953-6958.
12. A. Castellanos-Gomez, S. Bilan, L. A. Zotti, C. R. Arroyo, N. Agrait, J. C. Cuevas and G. Rubio-Bollinger, *Applied Physics Letters*, 2011, **99**, 123105-123116.
13. X. F. Guo, J. P. Small, J. E. Klare, Y. L. Wang, M. S. Purewal, I. W. Tam, B. H. Hong, R. Caldwell, L. M. Huang, S. O'Brien, J. M. Yan, R. Breslow, S. J. Wind, J. Hone, P. Kim and C. Nuckolls, *Science*, 2006, **311**, 356-359.
14. T. Li, J. R. Hauptmann, Z. Wei, S. Petersen, N. Bovet, T. Vosch, J. Nygård, W. Hu, Y. Liu and T. Bjørnholm, *Advanced Materials*, 2012, **24**, 1333-1339.
15. C. Jia, A. Migliore, N. Xin, S. Huang, J. Wang, Q. Yang, S. Wang, H. Chen, D. Wang and B. Feng, *Science*, 2016, **352**, 1443-1445.16.
16. M. Supur, C. Van Dyck, A. J. Bergren and R. L. McCreery, *Acs Applied Materials & Interfaces,* 2018, **10**, 6090-6095.
17. L. Liu, Q. Zhang, S. Tao, C. Zhao, E. Almutib, Q. Algaliby, S. W. Bailey, I. Grace, C. J. Lambert and J. Du, *Nanoscale*, 2016, **8**, 14507-14513.
18. Q. Zhang, L. Liu, S. Tao, C. Wang, C. Zhao, C. González, Y.J. Dappe, R. J. Nichols and L. Yang, *Nano Letters*, 2016, **16**, 6534−6540.
19. Q. Zhang, S. Tao, R. Yi, C. He, C. Zhao, W. Su, A. Smogunov, Y. J. Dappe, R. J. Nichols and L. Yang, *The Journal of Physical Chemistry Letters*, 2017, **8**, 5987-5992.
20. Z. Zhao and J. Gou, *Sci Technol Advanced Matererials*, 2009, **10**, 015005-01-015005-06.
21. G. Rubio-Bollinger, A. Castellanos-Gomez, B. Stefan, L. A. Zotti, C. R. Arroyo, A. Nicolás and C. J. Carlos, *Nanoscale Research Letters*, 2012, **7**, 254-01-254-04.
22. A. Castellanos-Gomez, N. Agrait and G. Rubio-Bollinger, *Nanotechnology*, 2010, **21**, 145702-01-145702-09.
23. B. Mann, H**.** Kuhn, *Journal of Applied Physics*, 1971, **42**, 4398-4405.
24. H. Yan, A. J. Bergren, R. Mccreery, M. L. Della Rocca, P. Martin, P. Lafarge and J. C. Lacroix, *Proceedings of the National Academy of Sciences of the United States of America*, 2013, **110**, 5326-5330.
25. S. Jang, P. Reddy, A. Majumdar and R. A. Segalman , *Nano Letters*, 2006, **6**, 2362-2367.
26. G. Heimel, L Romaner, E. Zojer, J.L. Bredas, *Accounts of Chemical Research*, 2008, **41**, 721-729.
27. C. González, E. Abad, Y. J. Dappe and J. C. Cuevas, *Nanotechnology,* 2016, **27**, 105201-01-105201-11.
28. J. C. Cuevas and E. Scheer, Molecular Electronics: an Introduction to Theory and Experiment; World Scientific: Singapore, 2010.

 